SKB

TECHNICAL REPORT 89-37

Alteration of natural UO_2 under oxidizing conditions from Shinkolobwe, Katanga, Zaire: A natural analogue for the corrosion of spent fuel

R J Finch, R C Ewing
Department of Geology, University of New Mexico

November 1989

SVENSK KÄRNBRÄNSLEHANTERING AB
SWEDISH NUCLEAR FUEL AND WASTE MANAGEMENT CO

BOX 5864 S-102 48 STOCKHOLM

TEL 08-665 28 00 TELEX 13108 SKB S
TELEFAX 08-661 57 19

ALTERATION OF NATURAL UO_2 UNDER OXIDIZING CONDITIONS FROM SHINKOLOBWE, KATANGA, ZAIRE: A NATURAL ANALOGUE FOR THE CORROSION OF SPENT FUEL

R J Finch, R C Ewing

Department of Geology, University of New Mexico

November 1989

ALTERATION OF NATURAL UO_2 UNDER OXIDIZING CONDITIONS FROM SHINKOLOBWE, KATANGA, ZAIRE: A NATURAL ANALOGUE FOR THE CORROSION OF SPENT FUEL

R. J. Finch
R. C. Ewing
Department of Geology
University of New Mexico

November 6, 1989

Submitted to
Radiochimica Acta
for
Proceedings of "Migration '89"

ABSTRACT

The alteration of uraninite (UO_{2+x}) at Shinkolobwe, Zaire provides a natural analogue for the corrosion of spent nuclear fuel in contact with oxidizing groundwater. Characterization of the uranium-containing solid alteration phases is required for predictive modeling of groundwater chemistries over long term periods of time. An integrated analysis of uraninite alteration products using optical microscopy, scanning electron microscopy (SEM), analytical electron microscopy (AEM), x-ray diffraction analysis (XRD), and electron microprobe analysis (EMPA) demonstrates the presence of coexisting phases at all analytical scales. The uranyl silicates (uranophane $(H_3O)_2Ca(UO_2)_2(SiO_4)_2{\cdot}3H_2O$ and cuprosklodowskite $(H_3O)_2Cu(UO_2)_2(SiO_4)_2{\cdot}4H_2O$) are ubiquitous in the samples studied and replace the Pb-uranyl oxide hydroxides (becquerelite $Ca(UO_2)_6O_4(OH)_6{\cdot}H_2O$, compriegnacite $K_2(UO_2)_6O_4(OH)_6{\cdot}8H_2O$, vandendriesscheite $PbU_7O_{22}{\cdot}22H_2O$, fourmarierite $PbU_4O_{13}{\cdot}6H_2O$, billietite $Ba(UO_2)_6O_4(OH)_6{\cdot}8H_2O$, and schoepite $UO_3{\cdot}2H_2O$) by reaction of the oxide hydrates with silica-rich groundwater. An overall reduction in grain size is apparent as alteration proceeds. Electron microscopy holds the greatest promise for the detailed characterization of the alteration products because of the extremely small sizes (< 1 micron to 5 microns) typical of the mineral grains.

Key Words: natural analogue, spent fuel, alteration, corrosion, uraninite, UO_2.

INTRODUCTION

Problems associated with the storage and disposal of spent nuclear fuel in geologic repositories have revitalized interest in the mineralogy and geochemistry of uranium compounds. The most common uranium mineral is uraninite (UO_{2+x}). Spent fuel from nuclear reactors is greater than 95 per cent UO_2. Hence, the study of uraninite and its alteration products provides valuable insight into the long-term behavior of spent fuel in the natural environment.

Modeling the long-term behavior of spent fuel in a geologic repository requires a thorough understanding of the solubility-controlling phases produced during the corrosion of the fuel; knowledge of the structures, chemistries, and thermodynamic stability of these secondary phases is crucial to any geochemical modeling program. The uranyl minerals occurring in Katanga, Zaire are numerous and varied . Some phases identified at Katanga have not been identified anywhere else in the world. This is due in part to the climate, savanna and open woodland with consistently warm temperatures and highly variable rainfall. At the Shinkolobwe mine, the uraninite-rich ore body is exposed at the surface to oxidizing meteoric waters. Exposure of spent nuclear fuel to such conditions would certainly be undesirable, but an understanding of the UO_{2+x} alteration products at Shinkolobwe is extremely useful for determining the U[VI] solubility-controlling phases that will be produced due to oxidative corrosion of spent fuel in a geologic repository.

This paper presents the preliminary results of a comprehensive study of uranyl phases produced by the oxidative alteration of uraninite from the Shinkolobwe mine. This study combines the results of phase characterization using optical microscopy, scanning electron microscopy (SEM), analytical electron microscopy (AEM), x-ray diffraction analysis (XRD), and electron microprobe analysis (EMPA). Such an approach provides a detailed mineralogical and geochemical description of the uranium phases present. Many of the analytical techniques

used in this study are not easily applied to the direct study of spent fuel due to its high radioactivity and toxicity. Spent fuel handled in a hot cell where applicable analytical techniques are extremely limited. The use of uraninite, shown to alter in an manner analogous to the alteration of spent fuel under disposal conditions, allows the use of analytical methods not available in a hot cell.

The Shinkolobwe deposit was selected for the following reasons: 1) Alteration occurs under suface oxidizng conditions (weathering) in a monsoonal-type environment (>100 cm rainfall per year) 2) The uraninite at Shinkolobwe is coarsely crystalline and lacks many of the impurities (e.g. Th, lanthanides) prevalent in many uranium deposits. The lack of impurities suggests that the thermodynamic stability of the Shinkolobwe ore may closely approximate that of spent fuel. The composition of "pure" Shinkolobwe uraninite is given (in weight percent) by Davis[1] as: UO_2 37.52, UO_3 52.77, PbO 7.02, He 0.159, N 0.076, Ce_2O_3 0.22, ZrO_2 0.14, $(Y,Er)_2O_3$ 0.35, $(La,Dy)_2O_3$ 0.153 (total: 98.408). The lead is entirely radiogenic. Uranium and its decay products constitute over 99 weight percent of the analytical total. Also, the high degree of crystallinity of the ore, verified by XRD and HRTEM analyses, limits diffusion paths unrelated to the microstructure of the uraninite. 3) The variety of uranyl minerals at Shinkolobwe[2] provides a unique opportunity to identify and characterize a large number of uranium phases which are of potential importance in modeling the long-term stability of spent nuclear fuel. The identification of coexisting phases and the determination of their paragenesis provides insight into stability relationships among phases. The identification of metastable versus stable phases is important to the interpretation of synthetic fuel corrosion studies because laboratory studies are of limited duration (metastable phases commonly form during laboratory studies).

Finally, this study demonstrates the need for an integrated analysis and characterization of uraninite alteration products by different techniques on the same sample (e.g. EMPA, SEM, AEM, HRTEM, and XRD). Such an approach provides information over a wide range of scales (millimeters to nanometers). Multiple phases coexist at all analytical scales.

NATURAL ANALOGUE STUDIES

Numerous studies have been conducted on the corrosion of spent UO_2 fuel under various parametric conditions.[3,4,5,6,7,8] These conditions vary from strongly oxidizing to strongly reducing in water chemistries ranging from deionized water to synthetic groundwater to concentrated brines. Early studies of uraninite dissolution were conducted for the purpose of concentrating uranium from uranium ore under conditions unlikely to be found in a nuclear waste repository. More recently, efforts to model UO_2 fuel dissolution based on natural analogues have gained momentum. To date, the focus of such studies, both natural and synthetic, is primarily on the solution chemistry, specifically, uranium concentrations in solution. The identification and characterization of solubility-controlling secondary uranium phases, especially as surface films on UO_2 fuel, has received detailed study only in the last five to six years.[9,10,11,12,13]

There are several problems in comparing the alteration of uraninite in natural systems to experimental studies with UO_2 fuel. For most ore deposits, the descriptive literature concentrates on the geology and mineralogy of the deposit. Characterization of groundwater composition is often of only minor (or no) interest to the exploration geologist. Characterization of the existing water chemistry in an ore body may give little insight into the conditions prevailing at the time of ore formation and subsequent alteration. Furthermore, the extreme complexity of natural systems, and the temporal and spatial variability of groundwater compositions (due to water-rock interactions which are incompletely understood) make thorough

analyses difficult and of limited use for comprehensive interpretation. Water-rock interactions may cause variations in solution composition by orders of magnitude over small distances (< 1 m). The oxidation potential of any aqueous system, of crucial importance to the oxidative dissolution of uraninite and UO_2 fuel, is difficult to quantify.

Natural analogue studies using uranium ore as a model for spent fuel disposal have focused on the concentrations of uranium and of the actinides in groundwater, often with scant attention to the uranium mineralogy of the deposit. Such studies are primarily concerned with the migration behavior of the actinides. However, it is the uranium minerals which control the concentration of uranium in uranium-rich solutions which are likely to be found in a high-level waste repository. Sunder and others[14] analyzed uranium minerals in a reducing environment and correlated their results to the uranium concentrations in the groundwater. There are, however, few natural analogue studies on uraninite exposed to an oxidizing environment. Correlating the results of geochemical models to actual groundwater chemistries requires a knowledge of the thermodynamic properties of the phases controlling solubility. Characterization of the uranyl minerals is an important step in this process. Only a few natural uranyl phases have been studied, however, and further work is required. In fact, the works of Puigdomenech and Bruno[15] and of Bruno and Sandino[9] on schoepite and rutherfordine are the most comprehensive thermodynamic studies on U[VI] phases to date. Schoepite, however, is not a common phase in contact with oxidized uraninite.

Corrosion studies of synthetic fuel have focused heavily on solution chemistry. This is due, in part, to the relative ease of solution chemistry analysis under controlled laboratory conditions. The pH is controlled chemically and Eh may be monitored or controlled by electrochemical means. Solid phases present on fuel surfaces, or solids present as precipitates or colloids in solution are usually poorly characterized. In addition, the duration of laboratory

experiments (up to eight or ten years) is limited compared to the geologic time periods required for waste isolation (>10,000 years). Phases precipitated on a UO_2 surface exposed to water for several months, or even years, may not represent true equilibrium phases. The kinetics controlling precipitation or recrystallization of U[VI] phases are also poorly understood.

The oxidation and corrosion of spent UO_2 fuel in a geologic repository should closely approximate the alteration of uraninite because of their structural and chemical similarities. Uraninite is generally more finely crystalline, is more oxidized, and contains more impurities than UO_2 fuel.

URANINITE ALTERATION

Uranium exists in two valence states in nature; the uranous ion, (U^{4+} or U[IV]) and the uranyl ion (U^{6+} or U[VI]). The chemistries of the two ions are dramatically different, owing to charge and size differences. Uranium, as U[IV] in uraninite (or synthetic UO_2), has a solubility in aqueous solutions on the order of 10^{-9} mol·kg^{-1}, making uraninite extremely stable in reducing environments. In more oxidizing environments, the uranyl ion solubility is potentially much higher, depending on the solution chemistry and the uranyl phases present. The oxidation potential (Eh) of an aqueous solution in contact with uraninite (or spent fuel) is of critical importance to the stability of UO_2 in groundwater. Much work has been done on the dissolution of both natural and synthetic UO_2 under oxidizing conditions. A knowledge of the stable phases in contact with oxidizing water offers much insight into the long-term behavior of UO_2 and its alteration products.

Uraninite (UO_{2+x}, $0 < x < 0.25$) is formed as stoichiometric UO_2 in the natural environment (most granitic pegmatite uraninite also contains significant amounts of thorium and lanthanides[16]). Due to post-depositional oxidation in a sedimentary environment, x is always

greater than zero in the formula UO_{2+x}.[17] Uraninite crystallizes in the cubic system (fluorite structure type, Fm3m). The oxidation of uraninite is due to oxygen diffusion into the cubic unit cell. The excess oxygen enters the unoccupied uranium equivalent interstices. At the oxidation state $UO_{2.25}$, there is one excess oxygen atom per uraninite unit cell.[18] The structure at the oxidation state $UO_{2.67}$ is orthorhombic. The phase change at $UO_{2.67}$ is reconstructive, and the uranium-oxygen coordination geometry changes from [8]-coordinate cubic to a [7]-coordinate pentagonal dipyramid.[19] This may be accomplished by the formation of $(UO_2)^{2+}$ at the surface followed by recrystallization to $UO_{2.67}$.[20] The structure of $UO_{2.67}$ is based on sheets of UO_7 polyhedra. Many uranyl hydroxides consist of stacking sequences of these sheets.

The only anhydrous uraninite oxidation products reported in nature are $UO_{2.25}$ and rarely $UO_{2.33}$ (as α-U_3O_7[21]). No anhydrous oxides above $UO_{2.33}$ are known to occur in nature. Further, the coexistence of $UO_{2.25}$ with the uranyl oxide hydrates, such as schoepite and clarkeite, in contact with oxidizing solutions, indicates that $UO_{2.25}$ is the anhydrous phase expected due to oxidative corrosion of spent UO_2 fuel. The existence of anhydrous oxidized layers on spent fuel having compositions above $UO_{2.33}$ (e.g $UO_{2.5}$, $UO_{2.67}$, UO_3) is often cited in the literature of spent fuel dissolution studies to explain solubility control.[20,3,22,23] The thickness postulated for such layers is 5-10 nm.[20] Ten nanometers is too thin to be detected by many analytical methods. In fact, such thicknesses are on the order of ten unit cells or less for $UO_{2.25}$ ($a = 0.5441$ nm). To date, these layers have not been observed directly. If such microlayers exist on spent fuel, similar phases should be present as domains in uraninite in contact with the uranyl oxide hydrates. Domains of such dimensions may be observed using HRTEM.

The most distinctive feature of all the uranyl oxide hydrates is the persistence of the $(UO_2)^{2+}$ unit in their structures.[24] The coherence of the $(UO_2)^{2+}$ unit in these structures explains the lack of substitution for uranium in the uranyl minerals by elements such as Th and the

lanthanides, which are common in most granitic pegmatite U[VI] minerals. For example, Hoekstra and Siegel report less than 0.05 wt.% La present in schoepite when synthesized using $La(OH)_3$ in solution.[24]

Gummite

The oxidative alteration due to weathering of uraninite is zonal. These zones are on the order of a few centimeters across. The innermost zone contains oxidized uraninite which is usually veined by U[VI] phases and is often partially hydrated. The uraninite in contact with the uranyl oxide hydrates generally shows a sharp x-ray diffraction pattern.[25] In some instances, the core is composed entirely of secondary minerals, the uraninite being completely replaced by the oxide hydrates or silicates. The core zone is surrounded by a mantle of generally fine-grained, and intimately intergrown uranyl-oxide hydrates and alkaline-earth uranyl oxide hydrates. The generic term for the commonly yellow-orange, fine-grained, waxy alteration rims found on many uranium ores is "gummite". Frondel[26] showed that gummite consists predominantly of uranyl oxide hydrates, lead-uranyl oxide hydrates and uranyl silicates. Less commonly uranyl phosphates and uranyl carbonates occur as constituents of gummite. Table 1 lists the zonation as described by Frondel.[26]

Table 1 **Zonation of Uraninite Alteration (after Frondel[26])**

ZONE	MINERALOGY	DOMINANT CATIONS (decreasing order of abundance)
Zone 1 (core)	uraninite	U^{4+}, U^{6+}, Pb
Zone 2	Pb-U oxide hydrates	U^{6+}, Ca, Pb, K, Na, Si, Ba
Zone 3	uranyl silicates	U^{6+}, Ca, Si, K, Na, Pb

The most common minerals in zone 2 are the Pb-bearing phases fourmarierite, vandendriesscheite, wölsendorfite, curite, calciouranoite, clarkeite, and the Pb-deficient phases

schoepite, becquerelite (Ca), and compreignacite (K).[26,27,28] Lead is enriched in zone 2 with respect to the uraninite. The essential lead in the Pb-uranyl oxide hydrates is derived from radiogenic lead in the primary uraninite. All uranyl minerals, however, contain some lead due to the radioactive decay of uranium in their structures.

Zone 3 consists predominantly of the calcium-uranyl silicates uranophane and beta-uranophane. In fact, uranophane is probably the most common U[VI] mineral in nature.[28] Other uranyl silicates reported by Frondel,[26] but with less frequency of occurrence are, kasolite (Pb), sklodowskite (Na and K), and soddyite. Cuprosklodowskite (Cu) is a relatively common alteration product in several copper-bearing localities such as the Katanga district of Zaire.[28] The formation of silicates is due to the reaction of the Pb-uranyl oxide hydrates with circulating groundwaters containing dissolved silica.

Lead content decreases sharply in zone 3 with respect to zone 2, due to leaching of Pb by groundwater. The only Pb-bearing uranyl silicate is kasolite, although minor Pb will substitute for Ca in the uranophane structure. Thorium and lanthanides content also decreases from the core outward and are virtually absent from the silicate phases in zone 3.[26,28] Calcium is the most common cation besides Pb in zone 2 and is the predominant cation in the zone 3 silicates. Sodium and potassium generally occur as minor constituents in the oxide hydroxides and uranyl silicates except in more saline environments.[17]

The zonation of altered uraninite may differ from the zonation listed in Table 2. For example, the entire uraninite crystal may be altered to silicates, or clarkeite may replace the uraninite completely at the core (zone 1). The type of alteration associated with gummite formation is consistent with weathering in an oxidizing environment in contact with meteoric water, although late-stage oxidizing hydrothermal fluids may lead to the formation of gummite.[29]

Other minerals commonly found in gummite include the uranyl carbonate rutherfordine and several uranyl phosphates.[26] Rutherfordine is often present as intergrowths with the uranyl minerals though it is not usually a major constituent. Rutherfordine also occurs as coatings due to evaporation of uranium-containing carbonate waters. The uranyl phosphates are often precipitated from solutions containing significant dissolved phosphorous. Langmuir[17] indicates that the uranyl phosphates are the most stable phases in contact with phosphate-rich groundwater, even when silica is present.

The alteration of natural uraninite in an oxidizing environment always produces a variety of minerals; never has a single, isolated phase been reported. These phases are generally microcrystalline and intimately intergrown, making positive identification difficult and often impossible. Hence, these minerals are often ill-defined. Phase relationships among the uranyl minerals are also poorly understood. Deliens[30] has reviewed uranyl mineralogy and phase associations at Shinkolobwe. His study is the most comprehensive to date. This study provides additional refinements to Deliens' work.

GEOLOGY AT SHINKOLOBWE

The mine at Shinkolobwe in the Katanga District, Shaba, Zaire is located in south central Africa. The climate is savanna and open woodland, receiving over 100 cm of rainfall in the six month wet season (November - April) and less than 12.5 cm of rain during the dry season (May - October). The ore body is exposed at the surface and extensive weathering has significantly altered, or in some cases replaced, the primary uraninite. The uranium mineralization occurs along brecciated fault and fracture zones. Meteoric waters have penetrated to depths of 80 meters or more.

The Shinkolobwe mine is located in the region of southeastern Zaire known as the Shaba Crescent (Figure 1). The Shaba Crescent represents the northern and western extent of the Lufilian Arc, folded and faulted sedimentary rocks with intrusive and extrusive structures present throughout. The southeastern end of the Lufilian arc is known as the Zambian copper Belt. Together, the Shaba Crescent and the Zambian Copper Belt comprise the South Equatorial cuprocobaltiferous metallogenic province, an area rich in copper, zinc, iron, lead, cobalt, cadmium, germanium, uranium, nickel, silver, barium, and gold. The basement rocks in Shaba are composed of approximately 1.2 billion year old (Upper Proterozoic) dolomitic shales and siltstones, siliceous dolostone, greywackes, and massive mudstones known as the Katanga system. The lowermost member of the Katanga System is the Roan Supergroup, consisting of dolomitic shales, siliceous dolostones and chloritic siltstones. The Roan supergroup was laid down in a large structural basin bounded to the east and northwest by converging mountain chains. The climate in the Late Proterozoic was hot and humid and the basin was covered wholly, or locally, by a shallow lagoonal sea. Dolomitic muds, algal reef complexes, and possibly evaporitic beds make up the 1500 m-thick Roan.[2]

Mineralization in the Shaba Crescent is located entirely within the "Mines Group" of the Roan supergroup. The Mines group is the oldest resistant dolomite complex in the Roan. The mineralization is found in two horizons at the base of the Mines Group. The lowest horizon is a siliceous dolomite 10 to 15 meters thick. Above this layer lies a barren algal dolomite 15 meters thick. Above this barren dolomite is a sandy dolomitic shale 5 to 10 meters thick. The Mines group is fragmented by numerous transverse faults and the outcrop pattern is sporadic.

During the period 700 million to 620 million years ago the Shaba area experienced tectonic movements related to an uplift in the south. The thrust faulting in the area is related to this event. This was also a thermal epoch, giving rise to the magmatic structures present in the

area. Due to mobilization of radiogenic lead at this time, most of the ores give ages corresponding to this time.[31] The thrust faults are cut by oblique faults, and it is along these thrust faults and oblique faults that much of the exposed Roan Group was brought to the surface as fragments of the original units. The breakup of the Roan is probably due to movement of the more plastic evaporite beds found in the basin.

Primary Mineralization and Alteration

The most prevalent and important ore in the Mines Group are the copper minerals, both primary and secondary. Mineralization in the Mines Group is not consistent. Some of the fragments in the Mines Group average up to approximately five weight percent copper. Other similar fragments may be barren of any ore. The origin of the primary mineralization has not been determined, but the mineralization may have been patchy within the Roan, depending on the local environment during, or immediately subsequent to, deposition. The primary copper minerals may have replaced syngenetic pyrite during diagenesis.

The host rocks (siliceous dolomites and shales) contribute to relatively high concentrations of silica in solution. Carbonate, from calcium- and magnesium-carbonate minerals, is also prevalent. Sulfur is derived from the alteration of several primary sulfides (e.g. cattierite, CoS_2; chalcopyrite, $CuFeS_2$; digenite, Cu_9S_5; linnaeite, Co_3S_4; and pyrite, FeS_2). Common uranyl complexes in solution at Shinkolobwe are therefore expected to be $[UO_2(CO_3)_2]^{2-}$, $[UO_2(CO_3)_3]^{4-}$, $[UO_2(SO_4]^{2-}$, and $[UO_2(SiO_4)]^{2-}$. Metal cations present are Ca^{2+}, Ba^{2+}, Mg^{2+}, Cu^{2+}, Pb^{2+}, Mo^{6+}, V^{5+}, and lanthanides (Ce^{3+}, La^{3+}, Y^{3+}, Gd^{3+}, Dy^{3+}).

The mineralization at Shinkolobwe does not follow stratification. Instead, it occurs as pods and veins filling fractures, faults and brecciated zones in the host rock. The Mines Group fragment which contains the ore body is surrounded by a chlorite-quartz breccia. The fragment

was probably brought to the surface as a result of the upward movement of the core. The uraninite mineralization is probably primary and occurs at the base of the lower ore horizon. Some remobilization of uranium and radiogenic lead occurred during the thermal events related to tectonism during the period 700 to 620 million years ago (Late Proterozoic to Early Paleozoic) and some lead loss occurred during later hydrothermal events (approx. 420 million years ago).[31] However, a magmatic origin for the uranium mineralization is not considered likely. Some of the uranium and lead may have been remobilized during this time, and the uraninite ages given for Shinkolobwe are on the order of 620 to 700 million years.[31] The individual ore bodies are generally small. Uranium-rich secondary mineralization, due to hydrothermal alteration and weathering of the primary uraninite, occurs along fractures and brecciated faults and is frequently separate from the primary ore body.

Secondary uranium mineralization in deep-seated veins or vugs may be related to hydrothermal events as a result of magmatism 620 to 700 million years ago. However, secondary mineralization due to surface alteration has occurred as a result of weathering conditions following exposure of the ore body at the surface due to uplift and erosion of the Roan Supergroup. The surface alteration at Shinkolobwe is probably Tertiary in age (<60 million years). Secondary galena is Tertiary in age.[2] Weathering of the ore body occurred along numerous fractures and veins. Some seams of uraninite in the ore zone have been completely altered. Passage of meteoric water along cellular siliceous rocks enhanced alteration in the deposit. Secondary mineralization is extensive and several occurrences exist away from the primary ore. The secondary deposits are often rich enough in uranium to be mined economically.

RESULTS

Optical Microscopy

Optical microscopy was employed for phase identification and for the determination of phase relationships. Resolution is on the order of tens of microns. The use of optical properties such as refractive index, pleochroism, optical sign and crystal habit provide preliminary identification of minerals in the prepared thin sections (identifications are often tentative until microprobe and x-ray diffraction analyses are completed). Classical optical work on uraninite alteration products is often unable to resolve the distinct phases present in the extremely fine-grained alteration rims which are simply identified as "gummite". However, many of the minerals present are relatively coarse grained (> 2 mm) and may be identified by optical techniques. The value of optical microscopy is that it allows the determination paragenetic relations among minerals. Features indicating replacement of pre-existing phases include embayed mineral grains and veining of euhedral grains. Such characteristics are prevalent in the samples studied. These observations are useful in estimating the relative stability of coexisting phases.

As the uraninite oxidizes and hydrates, a layer of various uranyl oxide hydrates forms. The phases most common are becquerelite, fourmarierite, vandendriesscheite, schoepite, billietite, and compriegnacite. These phases are similar in structure and optical properties, and significant solid solution may exist between end-member compositions.[28,35] Positive identification of individual phases requires EMPA and XRD.

Minute inclusions of acicular minerals, tentatively identified as uranyl silicate (uranophane ?), occur within the relatively coarse grained uranyl oxide hydrates. These inclusions are a few tens of microns long. Positive optical identification of these phases was not possible. Subsequent EMPA revealed the presence of silicon. Based on the euhedral nature of

both the host phase and the inclusions, the inclusions probably formed concurrently with the oxide hydrates, although the paragenetic relationship is not clear.

Veining of both the alteration rims and core uraninite is common and is due to fluid interaction with the preexisting minerals. The mineralogy is relatively homogeneous within each vein. The veins are on the order of 1-2 millimeters across and may span several centimeters. Mineralogically, there appears to be two types of veining. In one, uranyl silicates (uranophane or cuprosklodowskite) fill the vein and are derived from the oxide hydrates by reaction with silica-rich groundwater (Figure 2). The uranyl silicates are extremely fine grained and appear as fibrous mats having variable optical orientations. The surrounding coarser grained minerals are embayed or significantly replaced along the edge of the vein by the silicates. The silicate veins often cross into the uraninite without any change in mineralogy.

The second type of vein contains predominantly Pb-uranyl oxide hydrates.The grain size is significantly reduced with respect to earlier formed Pb-uranyl oxide hydrates. Grain sizes are relatively uniform within the vein and are usually on the order of a few tens of microns. Grain sizes are reduced across the vein/host interface in a gradational manner distinct from the clear replacement by the uranyl silicates mentioned above. The exact cause of this type of texture is not clear, but groundwater reactions are probably important. Minerals appearing in this second type of vein include fourmarierite, vandendriesscheite, curite, clarkeite, and masuyite (all high in lead relative to schoepite, becquerelite, and billietite). Fourmarierite and vandendriesscheite also occur as coarser grained constituents in the host alteration rim from which the finer-grained minerals are derived. This type of vein is potentially much larger than the silicate veins, and may range in size from less than 1 mm to 4 or 5 mm across. They often broaden to merge with the exterior coatings on the alteration rims which are also extremely fine-grained and constitute the traditional gummite.

Scanning Electron Microscopy (SEM)

Scanning electron microscopy is a useful tool for analyzing surface morphology, phase associations and for providing qualitative chemical analysis by energy dispersive spectroscopy (EDS). SEM work has been carried using a Hitachi S-450 SEM. Phase identification is based on crystal habit and EDS analysis, and is verified, when possible, with microprobe analysis and x-ray powder diffraction. Because of similarities in habit and the inability to determine molecular water or carbonate, many identifications are tentative. Elemental determinations below Z = 13 (Al) are not possible. The common occurrences of Mg-uranyl minerals (e.g. sklodowskite) at Shinkolobwe means that several tentative identifications may not include Mg phases, though Mg may be present. However, significant Mg has not yet been detected in these samples using EMPA.

Common minerals surrounding the uraninite, and often in contact with it, are becquerelite (most abundant), fourmarierite, vandendriesscheite, schoepite, and billietite. These minerals have similar morphologies, and the Pb-bearing phases have comparable chemistries. Euhedral crystals of these minerals are often covered by surface fines of uranyl silicates or carbonates (Figure 3a).

The presence of fine-grained uranyl silicates is evident to the limit of resolution (< 0.5 microns). The silicates are ubiquitous in the samples studied and occur most abundantly in veins. The uranyl silicates form fibrous matted coatings on their host minerals and are derived by reaction of silica-rich groundwater with the oxide hydrates. Ca is the most common cation present in the silicates (uranophane) although copper is commonly present (cuprosklodowskite). Uranophane is the most common secondary mineral found at Shinkolobwe.[2] Cuprosklodowskite and uranophane may coexist, but similarities in their structures suggests some solid solution between the end member compositions.

Other minerals detected include the Pb-bearing phases curite and masuyite, although these phases are most often present as small (< 1 micron) crystals in contact with the earlier-formed Pb-uranyl oxide hydrates (e.g. fourmarierite) or the uranyl silicates . Phases present as coarse-grained crystals are also common constituents of the finer-grained veins. The reduction of grain size across the vein interface is evident in Figure 3c.

The uranyl sulfates and carbonates are the most soluble uranyl oxides. These phases are relatively common at Shinkolobwe, though they do not occur in large quantities. Rutherfordine is present in the alteration rims as small, acicular crystals of variable length (5 to 50 microns, figure 3d). The exact paragenesis is unclear at this time, although it is likely that rutherfordine precipitates during periods of reduced groundwater flow. Figure 3d also illustrates the coexistence of multiple phases (rutherfordine, uranophane, becquerelite) at a small scale.

Analytical Electron Microscopy (AEM)

Analytical electron microscopy includes TEM, HRTEM, electron diffraction, and EDS. TEM can be used to observe crystal habits and phase relationships. TEM and HRTEM are also the methods best suited for the observation of the transitionally oxidized areas such as $UO_{2.5}$ or anhydrous $UO_{2.67}$ and UO_3 that have been proposed in spent fuel solubility studies (if these layers or domains exist). The HRTEM is used to observe grain and subgrain boundaries, possible radiation damage, and crystallite size. Electron diffraction is used in conjunction with HRTEM to determine crystallinity and, in conjunction with EDS, aids in phase identification. Chemical detection is not possible for elements below Z = 11 (Na) using EDS. Structural similarities between phases means that many identifications are tentative, especially since structural water cannot be determined. Transmission electron microscopy and high-resolution transmission electron microscopy were performed on crushed fragments on holey-carbon grids using the

JEOL2000 FX TEM operated at 200 kV. Phase compositions were determined using a Tracor TN5500 EDS.

The effect of alpha-decay damage in the secondary minerals is not readily obvious. The uranyl minerals observed show a high degree of crystallinity; thus, annealing of radiation-damaged areas is probably rapid. The migration of radiation-damage induced defects may be related to the observed reduction in grain size of phases such as fourmarierite or vandendriesscheite. Also, many of the secondary phases may be relatively recent and would lack a significant accumulation of defects. Figure 4 is a bright-field image of a uranyl oxide hydrate, probably schoepite. The image shows a mottled diffraction contrast which may be due to radiation damage.

X-ray Diffraction (XRD)

X-ray diffraction offers the most definitive method of phase identification. Minerals tentatively identified using optical microscopy are verified with x-ray powder diffraction. However, the minerals schoepite, becquerelite, billietite, fourmarierite, and to some extent vandendriesscheite, have similar x-ray diffraction patterns. EMPA is often required to more confidently distinguish between these phases. Also, comprehensive x-ray data on the uranyl minerals is limited or unavailable, making identification based on standard search techniques difficult or impossible. Several diffraction patterns obtained on yellow material collected from "gummite" rims correspond to the synthetic phase α-$UO_3 \cdot 0.8H_2O$. The presence of $UO_3 \cdot 0.8H_2O$ may be due to dehydration of schoepite during storage. Hoekstra and Siegel[8] synthesized α-$UO_3 \cdot 0.8H_2O$ by the dehydration of natural schoepite. X-ray powder diffraction patterns are collected with the SCINTAG X-ray Diffractometer ($Cu_{K\alpha 1}$ radiation, λ=0.15406 nm; nickel filter) and Debeye-Scherrer cameras for microscopically small samples.

Crystallite size effects the x-ray powder diffraction pattern. Broad peaks result from poorly crystalline samples or small crystallite size. Uraninite is commonly deposited as fine-grained aggregates, "pitchblende". Crystallite size may also be reduced due to annealing of radiation damage. Small grain size enhances the oxidation of UO_2 by supplying additional diffusion paths for oxygen and water. X-ray diffraction data have been obtained on unaltered uraninite and on uraninite in contact with the oxide hydrates. Both of the uraninite samples show relatively sharp diffraction maxima and closely match the pattern obtained from a reagent grade sample of UO_2 powder (although the synthetic material has probably undergone some oxidation and likely represents $UO_{2.25}$). Such sharp difraction maxima indicate a high degree of crystallinity. Intensities are reduced in the diffraction patterns obtained on the uraninite samples compared to those of the synthetic UO_2.

Table 2 **Uranyl minerals identified in this study (to date)**

OXIDE HYDRATES	
schoepite*	$UO_3 \cdot 2H_2O$
rutherfordine	UO_2CO_3
becquerelite	$Ca(UO_2)_6O_4(OH)_6 \cdot H_2O$
billietite	$Ba(UO_2)_6O_4(OH)_6 \cdot 8H_2O$
compriegnacite	$K_2(UO_2)_6O_4(OH)_6 \cdot 8H_2O$
clarkeite	$(Na,Ca,Pb)U_2(O,OH)_7$
curite	$Pb_2U_5O_{17} \cdot 4H_2O$
fourmarierite	$PbU_4O_{13} \cdot 6H_2O$
masuyite	$Pb_3U_8O_{27} \cdot 10H_2O$
vandendriesscheite	$PbU_7O_{22} \cdot 22H_2O$
SILICATES	
uranophane	$(H_3O)_2Ca(UO_2)_2(SiO_4)_2 \cdot 3H_2O$
cuprosklodowskite	$(H_3O)_2Cu(UO_2)_2(SiO_4)_2 \cdot 4H_2O$

*The phase α-$UO_3 \cdot 0.8H_2O$ is assumed to be dehydrated schoepite (Hoekstra and Siegel[8]).

DISCUSSION

The use of optical microscopy SEM, AEM, XRD, and EMPA shows multiple alteration products at all scales. Table 2 lists the uranyl minerals identified in this study. Becquerelite is the most common uranyl oxide hydrate in these samples. Becquerelite occurs as coarsely-crystalline aggregates of radiating crystals one to three millimeters long. The XRD powder patterns of billietite and compriegnacite are similar to the becquerelite powder patterns and identification is based on EMPA. Billietite and compriegnacite occur as intergrowths with becquerelite in the coarse-grained portions of the alteration rims. Several XRD powder patterns corresponding to α-$UO_2(OH)_2$ are attributed to schoepite that has undergone dehydration.[8] Schoepite is present most commonly as fine-grained, powdery material in contact with the coarse-grained becquerelite and uraninite.

The Pb-uranyl oxide hydrates, vandendriesscheite and foumarierite, occur as both coarse-grained constituents of the alteration rims and as fine-grained material within the Pb-rich veins. Vandendriesscheite, the most abundant coarse-grained Pb-uranyl mineral, is most commonly associated with becquerelite and uraninite. Curite and masuyite are present only as fine-grained constituents of the Pb-rich veins. The lead-uranium ratio in the Pb-uranyl oxide hydrates increases in the sequence vandendriesscheite → fourmarierite → masuyite → curite. This sequence also agrees well with the observed reduction in grain sizes for the Pb minerals. Theoretically, the Pb end-member clarkite contains the highest ratio Pb:U (= 1:2). Clarkeite occurs most commonly as powdery material on the exterior of the alteration rims or within cavities in the gummite.

The uranyl silicates are the most common uranyl minerals present. Uranophane is the most abundant, but cuprosklodowskite is also common. Both these phases occur as extremely fine-grained material in veins and as powdery coatings. The silicates replace the Pb-uranyl oxide

hydrates by reaction with the groundwater with a concomitant reduction in grain size. The presence of the Ca-uranyl silicates (e.g. uranophane) may be expected given the host rock mineralogy. The concentration of silica in equilibrium with uranophane is 60 ppm.[4] This is the silica concentration in equilibrium with amorphous silica. The groundwater composition at Shinkolobwe is complex, but will be dominated by the complexes $Si(OH)_4^0$, HCO_3^{2-}, SO_4^{2-}, and the cations Ca^{2+} and Mg^{2+}. These ions will be common in many geologic repository environments. Hence, there is reason to expect that the alteration of the uraninite at Shinkolobwe may closely approximate the long-term corrosion of spent fuel in a geologic repository exposed to oxdizing groundwater. Uranyl phases identified in studies of spent nuclear fuel corrosion are soddyite $[(UO_2)(SiO_4)_2 \cdot 2H_2O]$, schoepite, and uranophane and are only a fraction of the potential number of uranyl phases possible in a geologic environment.

CONCLUSIONS

This paper summarizes previous work on the oxidation and alteration of uraninite and synthetic UO_2 and presents some preliminary results from a study of uraninite alteration at Shinkolobwe. Even at the early stages of study, some conclusions may be drawn. Table 2 lists the uranyl minerals identified in this study. The total number of secondary uranyl minerals identified at Shinkolobwe is over 50.[2]

1) Becquerelite, vandendriesscheite, fourmarierite, schoepite, billietite, and compriegnacite, are most commonly the first formed phases at the surface of the uraninite. These phases have similar structures and significant solid-solution may exist among them.

2) The earliest formed phases are often replaced by much finer-grained phases such as curite and masuyite. Fourmarierite and vandendriesscheite are also common constituents within the fine-grained areas. These replacement minerals are generally higher in Pb than the coarser-grained minerals. The fine-grained areas occur as veins within the coarser grained minerals. The fine-grained material constitutes the traditional gummite.

3) Uranyl silicates replace the more coarse-grained minerals along veins. The exact paragenetic relationship between the fine-grained Pb-uranyl oxide hydrates and the silicates is not readily determined, although there is reason to believe that the silicates replace these minerals as siliceous groundwater reacts with the oxide hydrates. The uranyl silicates also occur as intimately intergrown crystals within the oxide hydrates. These silicate inclusions appear to be formed concurrently with the oxide hydrates and not by replacement. The uranyl silicates appear to be the most stable long-term phases due to alteration of uraninite exposed to oxidizing siliceous groundwater.

4) An overall reduction in grain size is apparent from the uraninite (core) outwards. This recrystallization takes place most commonly along veins rather than as easily identifiable concentric zones.

5) Due to the extremely small grain size, AEM holds the most promise for characterizing many of these minerals, and for determining paragenetic relations.

The long-term extrapolation of the behavior of spent fuel exposed to groundwater under oxidizing conditions requires the identification of the solid phase alteration products. The detailed examination of the alteration products of uraninite at Shinkolobwe provides exactly this

type of information. The sheer volume of uraninite alteration products at Shinkolobwe offers a unique opportunity to study many uranyl minerals at a single location. The alteration products were formed over periods of time in excess of millions of years. The low radioactivity of natural samples means that they can be more easily examined by the full range of analytical techniques available (e.g. EMPA, XRD, SEM, AEM, HRTEM). Thus, solid phases may be explicitly identified and their paragenesis determined.

Acknowledgements

AEM, SEM, and EMPA were performed at the Electron Microbeam Analysis Facility of the Geology Department and Institute of Meteoritics at the University of New Mexico. This paper benefited from critical reviews by Ray Eby and Janucs Januczek. Mark Miller assisted with XRD and general advice. This work was supported by Svensk Kärnbränslehantering AB (SKB).

REFERENCES

1 Davis, C. W.: The composition and age of uranium minerals from Katanga, South Dakota, and Utah. Amer. Journ. Sci., **11**, 201 (1926).

2 Gauthier, G., François, A. Deleins, M., Piret, P.: The uranium deposits of the Shaba Region, Zaire. Miner. Record, **20**, 265 (1989).

3 Ollilia, K.: Dissolution of UO_2 at various parametric conditions: A comparison between calculated and experimental results. In: *Scientific Basis for Nuclear Waste Management XII* (W. Lutze and R. C. Ewing, eds.) Mat. Res. Soc. Symp. Proc. Vol. 127, MRS, Pittsburgh 1989.

4 Bruno, J., Casas, I. Lagerman, B. Lagerman, B., Munoz, M.: The determination of the solubility of amorphous $UO_{2(S)}$ and the mononuclear hydrolysis constants of uranium(IV) at 25°C. In: *Scientific Basis for Nuclear Waste Management* (J. K. Bates and W. S. Seefelt, eds.) Mat. Res. Soc. Symp. Proc. Vol 84, MRS, Pittsburgh 1987

5 Christensen, H., and Bjerbakke, A.: Radiation induced dissolution of UO_2. In: *Scientific Basis for Nuclear Waste Management* (J. K. Bates and W. S. Seefelt, eds.) Mat. Res. Soc. Symp. Proc. Vol 84, MRS, Pittsburgh 1987.

6 Forsyth, R. S., Werme, L. O., Bruno, J.: The corrosion of spent UO_2 fuel in synthetic groundwater. J. Nucl. Mater., **138**, 1 (1986).

7 Bailey, M. G., Johnson, L. H., Shoesmith, D. W.: The effects of the alpha-radiolysis on the corrosion of UO_2. Corr. Sci., **25** (1985)

8 Thomas, G. F. and Till, G.: The dissolution of unirradiated UO_2 fuel pellets under simulated disposal conditions. Nucl. Chem. Waste Man., **5**, 141(1984).

9 Bruno, J. and Sandino, A.: The solubility of amorphous and crystalline schoepite in neutral to alkaline aqueous solutions. In: *Scientific Basis for Nuclear Waste Management XII* (W. Lutze and R. C. Ewing, eds.) Mat. Res. Soc. Symp. Proc. Vol. 127, MRS, Pittsburgh 1989.

10 Franco, P.,Trocellier, P., Menes, F.: UO_2 corrosion study in mineral water: A surface analysis approach. In: *Scientific Basis for Nuclear Waste Management XII* (W. Lutze and R. C. Ewing, eds.) Mat. Res. Soc. Symp. Proc. Vol. 127, MRS, Pittsburgh (1989).

11 Lahalle, M. P., Kruppa, J. C., Guillaumont, R., Genet, M., Allen, G. C., Holmes, N. R.: Surface analysis of UO_2 leached in mineral water studied by x-ray photoelectron spectroscopy. In: *Scientific Basis for Nuclear Waste Management XII* (W. Lutze and R. C. Ewing, eds.) Mat. Res. Soc. Symp. Proc. Vol. 127, MRS, Pittsburgh 1989.

12 Sunder, S., Shoesmith, D. W., Christensen, H., Bailey, M. G., Miller, N. H.: Electrochemical and x-ray photoelectron spectroscopic studies of UO_2 fuel oxidation by specific radicals formed during radiolysis of groundwater. In: *Scientific Basis for Nuclear Waste Management XII* (W. Lutze and R. C. Ewing, eds.) Mat. Res. Soc. Symp. Proc., Vol. 127, MRS, Pittsburgh (1989).

13 Uziemblo, N. H., Thomas, L. E., Shoenlein, L. H., Mastel, B., Jensen, E. D.: Solids characterizaton from hydrothermal tests with spent fuel. In: *Scientific Basis for Nuclear Waste Management X* (J. K. Bates and W. S. Seefelt, eds.) Mat. Res. Soc. Symp. Proc. Vol 84, MRS, Pittsburgh 1987.

14 Sunder, S., Taylor, P., Cramer, J. J.: XPS and XPS studies of uranium rich minerals from Cigar Lake, Saskatchewan. In: *Scientific Basis for Nuclear Waste Management XI* (M. J. Apted and R. E. Westerman, eds.) Mat. Res. Soc. Symp. Proc. Vol 112, MRS, Pittsburgh 1988.

15 Puigdomenech, I and Bruno, J.: Modelling uranium solubilities in aqueous solutions: Validation of a thermodynamic data base for the EQ3/6 geochemical codes. SKB Technical Report 88-21 (1988).

16 Berman, R.M.: The role of lead and excess oxygen in uraninite. Am. Min., **42**, 705 (1957).

17 Langmuir, D.: Uranium solution-mineral equilibria at low temperatures with applications to sedimentary ore deposits. Geochim. Cosmochim. Acta, **42**, 547 (1978).

18 Willis, B. T. M.: The defect structure of hyperstoichiometric uranium dioxide. Acta Crystallogr., **A34**, 88 (1978).

19 Loopstra, O.: Neutron diffraction investigation of U_3O_8. Acta Crystallogr., **17**, 651 (1964).

20 Johnson, L. H., and Shoesmith, D. W.: Spent fuel. In: *Radioactive Wasteforms for the Future* (W. Lutze and R. C. Ewing, eds.) Elsevier 1988.

21 Voultsidis, V. and Clasen, D.: Problems and boundary ranges of uranium mineralogy. Erzmetall., **31**, 3 (1978).

22 Johnson, L. H., Shoesmith, D. W., Lunansky, G. E., Bailey, M. G., Tremaine, P. R.,: Mechanisms of leaching and dissolution of UO2 fuel. Rad. Waste Man.,**56**, 238 (1982).

23 Nichol, M. J., and Needes, C. R. S.: The anodic dissolution of uranium dioxide-I. In perchlorate solutions. Electrochim. Acta, **20**, 585 (1975).

24 Hoekstra, H.R., and Siegel, S.: The uranium trioxide-water system. J. Inor. Nucl. Chem., **35**, 761 (1973).

25 Smith, D. K., Scheetz, B. E., Anderson, C. A. F., Smith, K. L.: Phase relations in the uranium-oxygen-water system and its significance on the stability of nuclear waste forms. Uranium, **1**, 79 (1982).

26 Frondel, C.: Mineral composition of gummite. Am. Min., **41**, 539 (1956).

27 Frondel, C.: Systematic mineralogy of uranium and thorium. Geol. Soc. Amer. Bulletin **1064**, 399 (1958).

28 Smith, D. K. Jr.: Uranium mineralogy. In: *Uranium Geochemistry, Mineralogy, Geology, Exploration, and Resources* (B. DeVivo, F. Ippolito, G. Capaldi, and P. R. Simpson, eds.), Inst. Min. Metall, 1984.

29 Ross, C. S., Henderson, E. P., Posnjak, E.: Clarkeite, a new uranium mineral. Am. Min.,**16**, 213 (1931).

30 Deliens, M.: Associations de minèraux secondaires d'uranium à Shinkolobwe (règion du Shaba, Zaïre). Bull. Soc. fr. Minèral. Crystallogr., **100**, 32 (1977).

31 Cahen, L., Snelling, N. J., Delhal, J., Vail, J. R.: *The geochronology and evolution of Africa*, Clarendon Press, Oxford, 1984, p.512.35Sobry, R.: Water and interlayer oxonium in hydrated uranates. Am. Min., **56**, 1065 (1971).

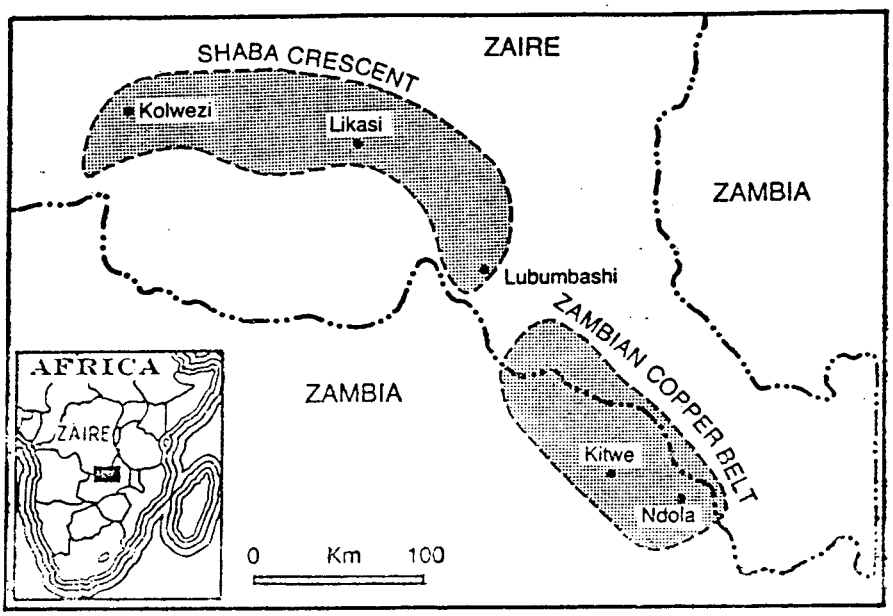

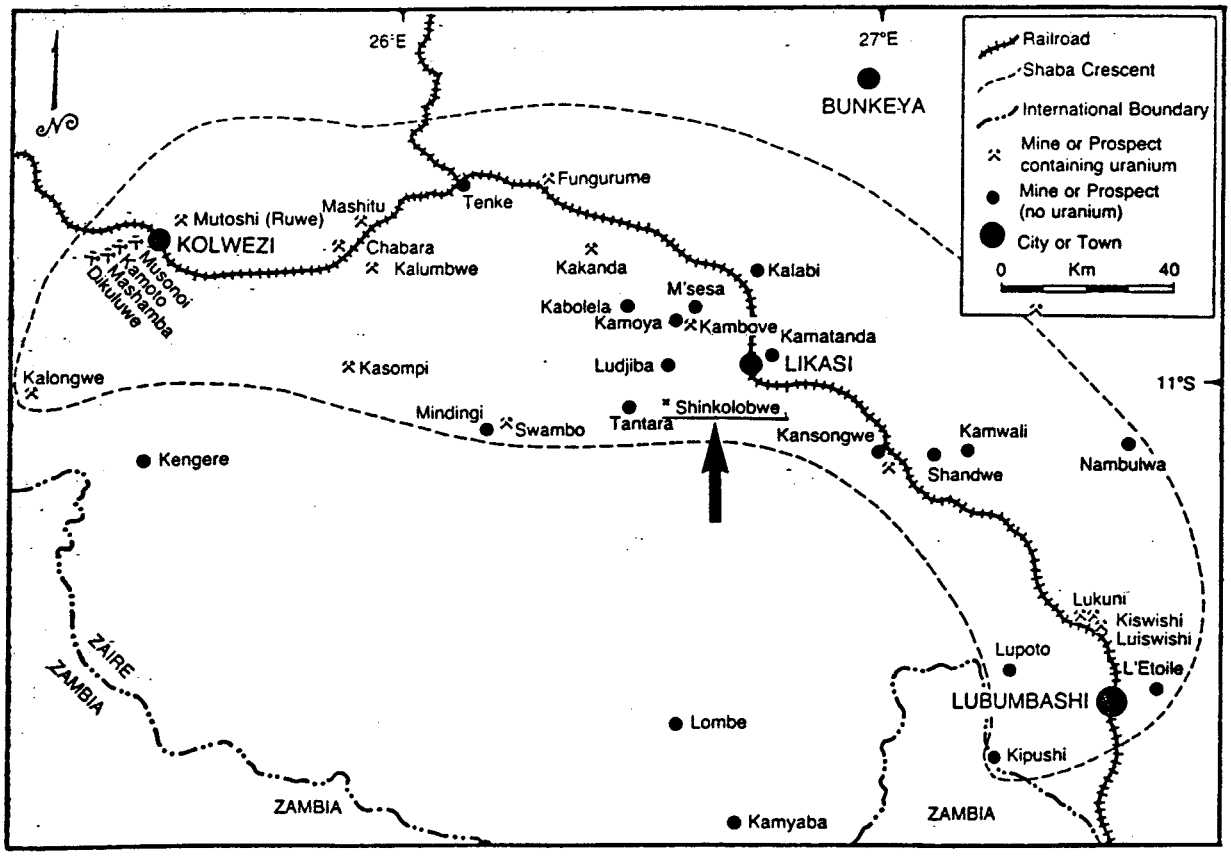

Figure 1 Map showing the location of Shinkolobwe mine in Katanga (Shaba), Zaire (From Gauthier *el al.*[12]).

Figure 2 Photomicrograph of uranyl silicate (S) replacing becquerelite (B) due to groundwater interaction. Scale bar equals 200 microns.

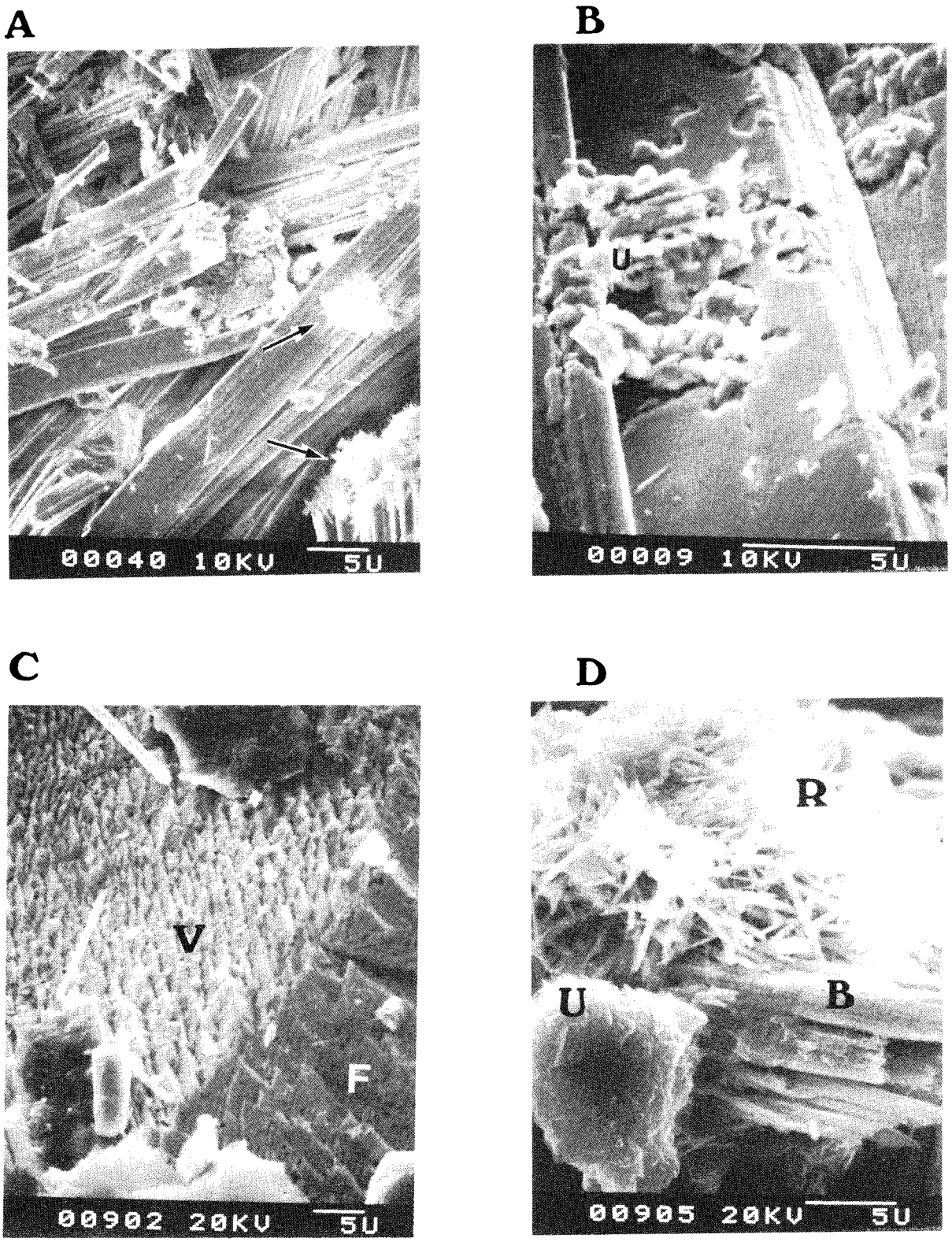

Figure 3 SEM micrographs of uraninite alteration. A) Euhedral becquerelite crystals with fine-grained rutherfordine (arrows). B) Becquerelite crystal being replaced by uranophane (U). C) Fourmarierite (F) veined by and being replaced by finer-grained Pb-uranyl oxide hydrates (V). The becquerelite shows a pitted surface characteristic of dissolution at the surface. Mats of an unidentified uranyl silicate are seen at the top and bottom of the image. D) Rutherfordine (R) and uranophane (U) with embayed crystals of becquerelite (B). The becquerelite is being replaced by uranophane.

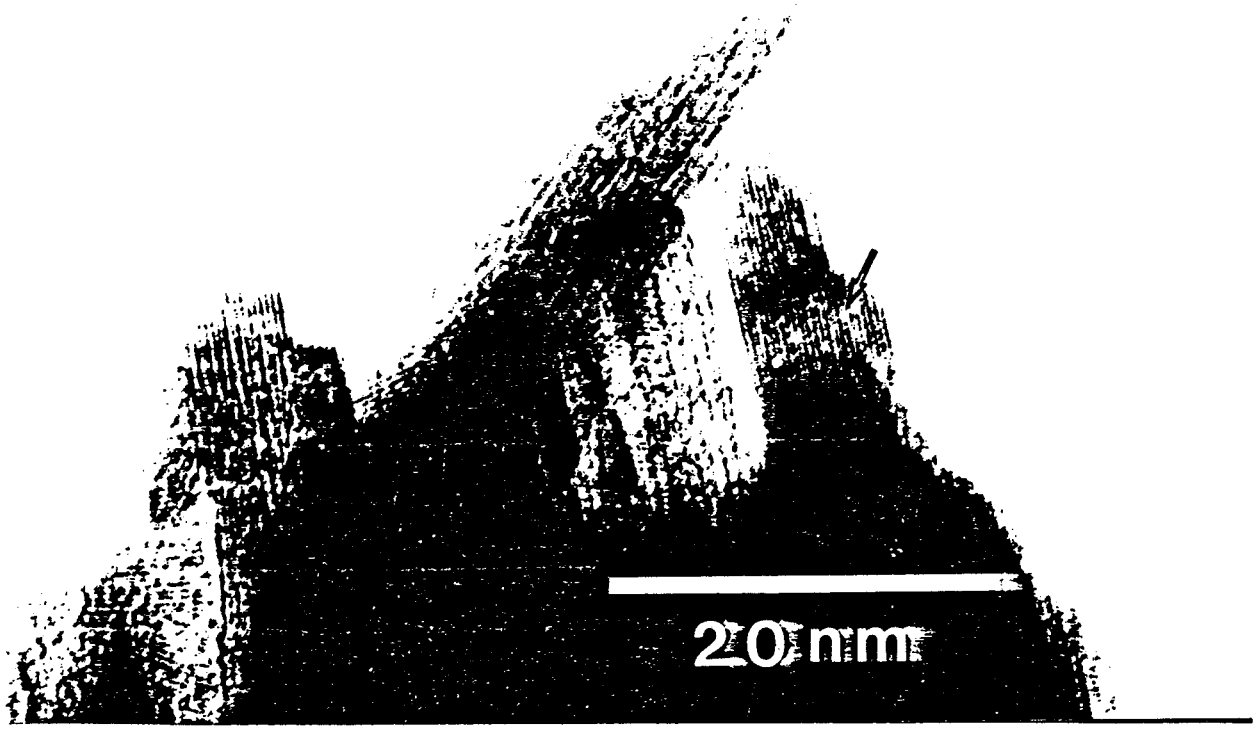

Figure 4 HRTEM micrograph of submicron-sized schoepite grains. Inset shows electron diffraction pattern characteristic of polycrystalline material. Some crystals are less than 10 nm across. Mottled diffraction contrast (arrow) may be due to radiation damage.

List of SKB reports

Annual Reports

1977–78
TR 121
KBS Technical Reports 1 – 120.
Summaries. Stockholm, May 1979.

1979
TR 79–28
The KBS Annual Report 1979.
KBS Technical Reports 79-01 – 79-27.
Summaries. Stockholm, March 1980.

1980
TR 80–26
The KBS Annual Report 1980.
KBS Technical Reports 80-01 – 80-25.
Summaries. Stockholm, March 1981.

1981
TR 81–17
The KBS Annual Report 1981.
KBS Technical Reports 81-01 – 81-16.
Summaries. Stockholm, April 1982.

1982
TR 82–28
The KBS Annual Report 1982.
KBS Technical Reports 82-01 – 82-27.
Summaries. Stockholm, July 1983.

1983
TR 83–77
The KBS Annual Report 1983.
KBS Technical Reports 83-01 – 83-76
Summaries. Stockholm, June 1984.

1984
TR 85–01
Annual Research and Development Report 1984
Including Summaries of Technical Reports Issued during 1984. (Technical Reports 84-01–84-19)
Stockholm June 1985.

1985
TR 85-20
Annual Research and Development Report 1985
Including Summaries of Technical Reports Issued during 1985. (Technical Reports 85-01-85-19)
Stockholm May 1986.

1986
TR 86-31
SKB Annual Report 1986
Including Summaries of Technical Reports Issued during 1986
Stockholm, May 1987

1987
TR 87-33
SKB Annual Report 1987
Including Summaries of Technical Reports Issued during 1987
Stockholm, May 1988

1988
TR 88-32
SKB Annual Report 1988
Including Summaries of Technical Reports Issued during 1988
Stockholm, May 1989

Technical Reports

1989

TR 89-01
Near-distance seismological monitoring of the Lansjärv neotectonic fault region Part II: 1988
Rutger Wahlström, Sven-Olof Linder, Conny Holmqvist, Hans-Edy Mårtensson
Seismological Department, Uppsala University, Uppsala
January 1989

TR 89-02
Description of background data in SKB database GEOTAB
Ebbe Eriksson, Stefan Sehlstedt
SGAB, Luleå
February 1989

TR 89-03
Characterization of the morphology, basement rock and tectonics in Sweden
Kennert Röshoff
August 1988

TR 89-04
SKB WP-Cave Project
Radionuclide release from the near-field in a WP-Cave repository
Maria Lindgren, Kristina Skagius
Kemakta Consultants Co, Stockholm
April 1989

TR 89-05
SKB WP-Cave Project
Transport of escaping radionuclides from the WP-Cave repository to the biosphere
Luis Moreno, Sue Arve, Ivars Neretnieks
Royal Institute of Technology, Stockholm
April 1989

TR 89-06
SKB WP-Cave Project
Individual radiation doses from nuclides contained in a WP-Cave repository for spent fuel
Sture Nordlinder, Ulla Bergström
Studsvik Nuclear, Studsvik
April 1989

TR 89-07
SKB WP-Cave Project
Some Notes on Technical Issues
Part 1: Temperature distribution in WP-Cave: when shafts are filled with sand/water mixtures
Stefan Björklund, Lennart Josefson
Division of Solid Mechanics, Chalmers University of Technology, Gothenburg, Sweden
Part 2: Gas and water transport from WP-Cave repository Luis Moreno, Ivars Neretnieks
Department of Chemical Engineering, Royal Institute of Technology, Stockholm, Sweden
Part 3: Transport of escaping nuclides from the WP-Cave repository to the biosphere. Influence of the hydraulic cage
Luis Moreno, Ivars Neretnieks
Department of Chemical Engineering, Royal Institute of Technology, Stockholm, Sweden
August 1989

TR 89-08
SKB WP-Cave Project
Thermally incuded convective motion in groundwater in the near field of the WP-Cave after filling and closure
Polydynamics Limited, Zürich
April 1989

TR 89-09
An evaluation of tracer tests performed at Studsvik
Luis Moreno[1], Ivars Neretnieks[1], Ove Landström[2]
[1] The Royal Institute of Technology, Department of Chemical Engineering, Stockholm
[2] Studsvik Nuclear, Nyköping
March 1989

TR 89-10
Copper produced from powder by HIP to encapsulate nuclear fuel elements
Lars B Ekbom, Sven Bogegård
Swedish National Defence Research Establishment
Materials department, Stockholm
February 1989

TR 89-11
Prediction of hydraulic conductivity and conductive fracture frequency by multivariate analysis of data from the Klipperås study site
Jan-Erik Andersson[1], Lennart Lindqvist[2]
[1] Swedish Geological Co, Uppsala
[2] EMX-system AB, Luleå
February 1988

TR 89-12
Hydraulic interference tests and tracer tests within the Brändan area, Finnsjön study site The Fracture Zone Project – Phase 3
Jan-Erik Andersson, Lennart Ekman, Erik Gustafsson, Rune Nordqvist, Sven Tirén
Swedish Geological Co, Division of Engineering Geology
June 1988

TR 89-13
Spent fuel
Dissolution and oxidation
An evaluation of literature data
Bernd Grambow
Hanh-Meitner-Institut, Berlin
March 1989

TR 89-14
The SKB spent fuel corrosion program
Status report 1988
Lars O Werme[1], Roy S Forsyth[2]
[1] SKB, Stockholm
[2] Studsvik AB, Nyköping
May 1989

TR 89-15
Comparison between radar data and geophysical, geological and hydrological borehole parameters by multivariate analysis of data
Serje Carlsten, Lennart Lindqvist, Olle Olsson
Swedish Geological Company, Uppsala
March 1989

TR 89-16
Swedish Hard Rock Laboratory – Evaluation of 1988 year pre-investigations and description of the target area, the island of Äspö
Gunnar Gustafsson, Roy Stanfors, Peter Wikberg
June 1989

TR 89-17
Field instrumentation for hydrofracturing stress measurements
Documentation of the 1000 m hydrofracturing unit at Luleå University of Technology
Bjarni Bjarnason, Arne Torikka
August 1989

TR 89-18
Radar investigations at the Saltsjötunnel – predicitions and validation
Olle Olsson[1] and Kai Palmqvist[2]
[1] Abem AB, Uppsala, Sweden
[2] Bergab, Göteborg
June 1989

TR 89-19
Characterization of fracture zone 2, Finnsjön study-site
Editors: K. Ahlbom, J.A.T. Smellie, Swedish Geological Co, Uppsala
Part 1: Overview of the fracture zone project at Finnsjön, Sweden
K. Ahlbom and J.A.T. Smellie. Swedish Geological Company, Uppsala, Sweden.
Part 2: Geological setting and deformation history of a low angle fracture zone at Finnsjön, Sweden
Sven A. Tirén. Swedish Geological Company, Uppsala, Sweden.
Part 3: Hydraulic testing and modelling of a low-angle fracture zone at Finnsjön, Sweden
J-E. Andersson[1], L. Ekman[1], R. Nordqvist[1] and A. Winberg[2]
[1] Swedish Geological Company, Uppsala, Sweden
[2] Swedish Geological Company, Göteborg, Sweden
Part 4: Groundwater flow conditions in a low angle fracture zone at Finnsjön, Sweden
E. Gustafsson and P. Andersson. Swedish Geological Company, Uppsala, Sweden
Part 5: Hydrochemical investigations at Finnsjön, Sweden
J.A.T. Smellie[1] and P. Wikberg[2]
[1] Swedish Geological Company, Uppsala, Sweden
[2] Swedish Nuclear Fuel and Waste Management Company, Stockholm, Sweden
Part 6: Effects of gas-lift pumping on hydraulic borehole conditions at Finnsjön, Sweden
J-E- Andersson, P. Andersson and E. Gustafsson. Swedish Geological Company, Uppsala, Sweden
August 1989

TR 89-20
WP-Cave - Assessment of feasibility, safety and development potential
Swedish Nuclear Fuel and Waste Management Company, Stockholm, Sweden
September 1989

TR 89-21
Rock quality designation of the hydraulic properties in the near field of a final repository for spent nuclear fuel
Hans Carlsson[1], Leif Carlsson[1], Roland Pusch[2]
[1] Swedish Geological Co, SGAB, Gothenburg, Sweden
[2] Clay Technology AB, Lund, Sweden
June 1989

TR 89-22
Diffusion of Am, Pu, U, Np, Cs, I and Tc in compacted sand-bentonite mixture
Department of Nuclear Chemistry, Chalmers University of Technology, Gothenburg, Sweden
August 1989

TR 89-23
Deep ground water microbiology in Swedish granitic rock and it's relevance for radionuclide migration from a Swedish high level nuclear waste repository
Karsten Pedersen
University of Göteborg, Department of Marine microbiology, Gothenburg, Sweden
March 1989

TR 89-24
Some notes on diffusion of radionuclides through compacted clays
Trygve E Eriksen
Royal Institute of Technology, Department of Nuclear Chemistry, Stockholm, Sweden
May 1989

TR 89-25
Radionuclide sorption on crushed and intact granitic rock
Volume and surface effects
Trygve E Eriksen, Birgitta Locklund
Royal Institute of Technology, Department of Nuclear Chemistry, Stockholm, Sweden
May 1989

TR 89-26
Performance and safety analysis of WP-Cave concept
Kristina Skagius[1], Christer Svemar[2]
[1] Kemakta Konsult AB
[2] Swedish Nuclear Fuel and Waste Management Co
August 1989

TR-89-27
Post-excavation analysis of a revised hydraulic model of the Room 209 fracture, URL, Manitoba, Canada
A part of the joint AECL/SKB characterization of the 240 m level at the URL, Manitoba, Canada
Anders Winberg[1], Tin Chan[2], Peter Griffiths[2], Blair Nakka[2]
[1] Swedish Geological Co, Gothenburg, Sweden
[2] Computations & Analysis Section, Applied Geoscience Branch, Atomic Energy of Canada Limited, Pinawa, Manitoba, Canada
October 1989

TR 89-28
Earthquake mechanisms in Northern Sweden Oct 1987 — Apr 1988
Ragnar Slunga
October 1989

TR 89-29
Interim report on the settlement test in Stripa
Lennart Börgesson, Roland Pusch
Clay Technology AB, Lund
November 1989

TR 89-30
Seismic effects on bedrock and underground constructions. A literature survey of damage on constructions, changes in groundwater levels and flow, changes in chemistry in groundwater and gases
Kennert Röshoff
June 1989

TR 89-31
Interdisciplinary study of post-glacial faulting in the Lansjärv area Northern Sweden 1986–1988
Göran Bäckblom, Roy Stanfors (eds.)
December 1989

TR-89-32
Influence of various excavation techniques on the structure and physical properties of "near-field" rock around large boreholes
Roland Pusch
Clay Technology AB and Lund University of Technology and Natural Sciences, Lund
December 1989

TR 89-33
Investigation of flow distribution in a fracture zone at the Stripa mine, using the radar method, results and interpretation
Per Andersson, Peter Andersson, Erik Gustafsson, Olle Olsson
Swedish Geological Co., Uppsala, Sweden
December 1989

TR 89-34
Transport and microstructural phenomena in bentonite clay with respect to the behavior and influence of Na, Cu and U
Roland Pusch[1], Ola Karnland[1], Arto Muurinen[2]
[1] Clay Technology AB (CT)
[2] Technical Research Center of Finland, Reactor Laboratory (VTT)
December 1989

TR 89-35
The joint SKI/SKB scenario development project
Editor: Johan Andersson[1]
Authors: Johan Andersson[1], Torbjörn Carlsson[1], Torsten Eng[2], Fritz Kautsky[1], Erik Söderman[3], Stig Wingefors[1]
[1] Statens Kärnkraftsinspektion, SKI Stockholm, Sweden
[2] Svensk Kärnbränslehantering AB, SKB, Stockholm, Sweden
[3] ES-Konsult, Bromma, Sweden
December 1989

TR-89-36
^{14}C-Analyses of calcite coatings in open fractures from the Klipperås study site, Southern Sweden
Götan Possnert[1], Eva-Lena Tullborg[2]
[1] Svedberg-laboratoriet, Uppsala
[2] Sveriges Geologiska AB, Gothenburg
November 1989